Enantioselective Carbon Isotope Exchange

Michael G. J. Doyle,* [a, b] Odey Bsharat,* [a] Anna Sib,[b] Volker Derdau,§ [b] Rylan J. Lundgren§ [a]

[a] Department of Chemistry, University of Alberta, Edmonton, Alberta T6G 2G2, Canada

[b] Sanofi Germany, R&D, Integrated Drug Discovery, Isotope Chemistry, Industriepark Höchst, 65926 Frankfurt, Germany

* These authors contributed equally to this work

§ Corresponding author. Email: rylan.lundgren@ualberta.ca, volker.derdau@sanofi.com

Abstract

The synthesis of isotopically labeled organic molecules is vital for drug and agrochemical discovery and development. Carbon isotope exchange is emerging as a leading method to generate carbon-labeled targets, which are sought due to their enhanced stability in biological systems. While many bioactive small molecules bear carbon-containing stereocenters, direct enantioselective carbon isotope exchange reactions have not been established. We describe the first example of an enantioselective carbon isotope exchange reaction, where (radio)labeled α-amino acids can be generated from their unlabeled precursors in a single step using a chiral aldehyde mediator with isotopically labeled CO_2. Many proteinogenic and non-natural derivatives undergo enantioselective labeling, including the late-stage radiolabeling of complex drug targets.

Main Text

The isotopic labeling of organic compounds is a universal tool at the forefront of the life sciences which is continuously relied upon in the drug discovery, crop science, and medical imaging sectors (*1, 2*). Swapping a native isotope with a less abundant or radioactive tracer allows end-users to leverage the understanding of biochemical pathways and processes by following the fate of these tracers using mass spectrometry or by radiation analysis (*3*). Among conceptual ways to introduce non-abundant isotopes, hydrogen isotope exchange (HIE) is arguably the most enabling, whereby a *H atom from a readily available source ($*H_2$ or $*H_2O$) replaces a native C–H bond (Fig. 1A, * = non-abundant isotope) (*4*). Under appropriate conditions, HIE can be used to label complex molecules at a late stage (*4–8*), and in rare cases, introduce *H-labels at stereogenic centers by stereoretentive processes (*9–11*).

As a consequence of H-based labels suffering from drawbacks in applied settings often related to metabolic degradation, label wash-out, or large kinetic isotope effects, carbon isotope exchange (CIE) has emerged as a complimentary labeling technology providing rapid access to C-labeled targets (Fig. 1A) (*12–14*). Embedded in the structural backbone of organic molecules, carbon labels show greater biological stability compared to H-isotopomers, and the native molecular structure is not altered as with the addition of exotic labels such as ^{18}F (*15*). ^{14}C-radiolabeled organic compounds have proven irreplaceable in the clinical and agrochemical setting because they can be distinguished in complex matrices and are easily observed even at low specific activity values (*2*). CIE presents unique challenges compared to HIE, as transformations must selectively break C–C bonds, liberate a functionalized carbon unit, and recapture a labeled variant. Nonetheless, recent CIE methods have been used for the formation of C–*C bonds from isotopically labeled CO_2 (*16–22*), CO (*23*), and CN^- (*24, 25*). Since many biologically active small molecules contain carbon stereocenters, methods for enantioselective CIE would be of immediate value. The inherent reversibility of CIE reactions makes designing these reactions challenging because the bond which forms the stereocenter is repeatedly broken and reformed. Aside from a single stereoretentive example (*23*), processes that generate stereogenic C–*C bonds via CIE give racemic (or achiral) products.

Since α-amino acids are one of the key building blocks of life and are found embedded in many approved small molecule drugs and biologics (*26, 27*), there is a strong need for C-labeled α-amino acid targets. ^{14}C-labeled α-amino acids are now heavily relied upon in drug development, mainly for (pre)absorption, distribution, metabolism, and excretion (ADME) studies

(*28, 29*). We recently disclosed a racemic CIE method wherein α-amino acids are directly labeled from their native precursors by undergoing aldehyde-catalyzed carboxylation/decarboxylation in the presence of $*CO_2$ (Fig. 1B) (*22*). Our earlier work was inspired by the function of pyridoxal phosphate (PLP) dependent enzymes, which perform various transformations of amino acids including decarboxylations, eliminations, and stereochemical inversions. Chin and Kim have developed PLP-mimetic amino acid receptors such as **1**, which are designed to transform L-amino acids into D-amino acids through hydrogen bonding interactions with an axially chiral aldehyde (Fig. 1B) (*30–33*). We questioned whether we could employ these axially chiral aldehyde receptors in a simultaneous reversible carboxylation/decarboxylation/resolution manifold to realize an enantioselective CIE reaction. Here we show that under $*CO_2$ (* = 13, 14) the Chin-Kim aldehyde mediates the single step enantioselective synthesis of *C-labeled α-amino acids from their unlabeled precursors (Fig. 1C). The process accepts both amino acid stereoisomers, can be used for ^{13}C- or ^{14}C-labeling applications, and accommodates complex targets like the amino acid drug telotristat. Preliminary kinetic analysis suggests the reaction proceeds via a simultaneous carboxylate exchange/resolution pathway.

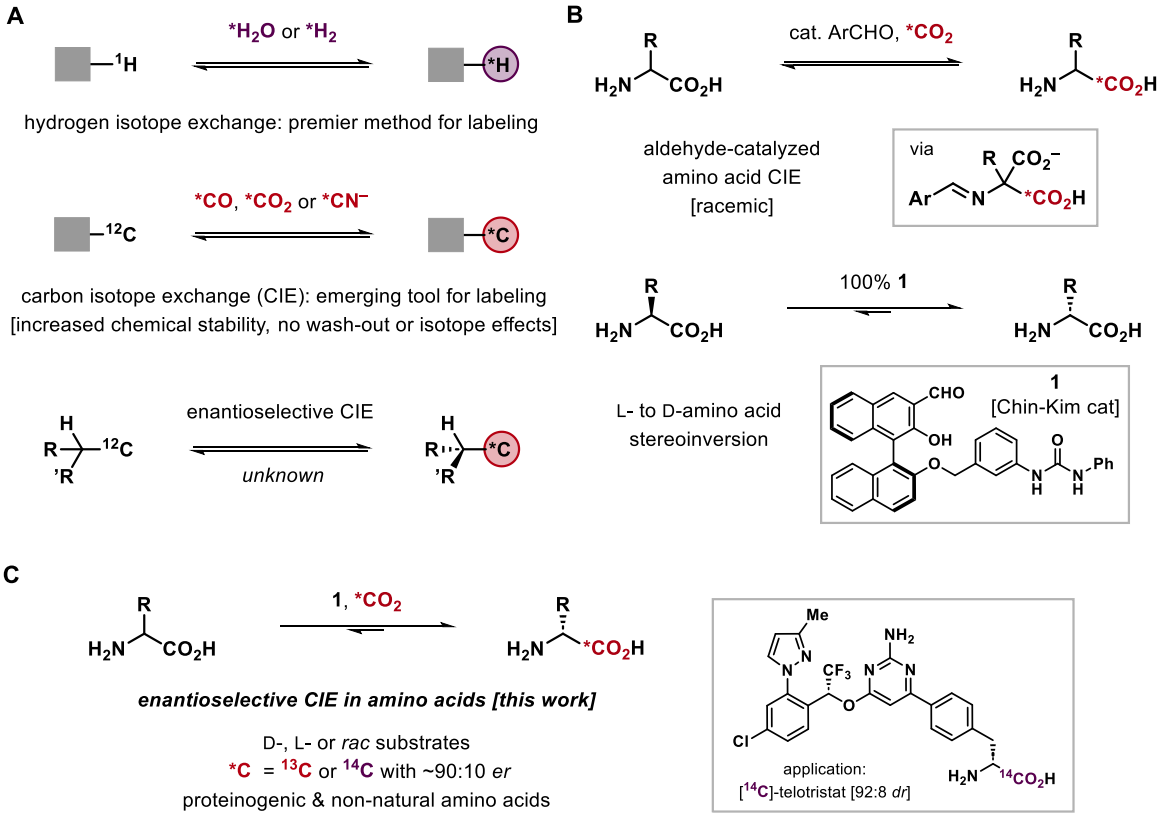

Fig. 1. Overview of CIE and relevant methods. (**A**) Current state-of-the-art in isotope exchange reactions. (**B**) Aldehyde-catalyzed carboxylate exchange in α-amino acids with $*CO_2$

and α-amino acid stereoinversion mediated by an axially chiral aldehyde. (**C**) Axially chiral aldehyde **1** mediates enantioselective CIE in α-amino acids with $*CO_2$. CIE = carbon isotope exchange.

The urea-tethered aldehyde **1**, first developed by Chin and Kim for L- to D-amino acid interconversions, mediates the enantioselective CIE of phenylalanine (**2**) to give the target in 65% yield, 71% ^{13}C incorporation and 90:10 enantiomeric ratio (*er*) when supplying ~4 equivalents of $[^{13}C]CO_2$ in DMSO, using DBU as a base (average of five runs). Figure 2A depicts how variations to the conditions and catalyst impacts reactivity. While **1** technically acts a catalyst and can be recovered from the reaction in high yield, using 20 mol% resulted in poor ^{13}C incorporation and *er*. The use of 2 equivalents of DBU was essential, as 1 equivalent of DBU or alternative bases resulted in reduced ^{13}C incorporation while yields and *er* remained high (see the SI for additional base effects). When starting from unlabeled racemic or L-**2**, similar rates of incorporation and resolution are observed, with similar terminal results (see the SI for kinetic analyses). Aldehyde **1** was the best performing mediator, while the analogous methyl ketone **C2** or thiourea species **C3** performed poorly. Variation of the aryl urea group had a minimal effect on incorporation or *er*, while variants of **1** without the urea linker gave only racemic product, including when in the presence of diphenylurea. Additionally, catalysts with point chirality such as aldehyde **C7** were unsuccessful in generating enantioenriched products (see the SI for a list of catalysts tested).

Once ^{13}C-labeled amino acid **2** is obtained, it can be readily upgraded as needed for specific applications that require either greater enantioenrichment or a larger extent of isotope incorporation (Fig. 2B). After using *(R)*-**1** in the enantioselective CIE reaction, D-α-amino acid oxidase (DAAO) can be subsequently employed in an enzymatic resolution to upgrade the *er* of labeled product to >99.5:0.5 (*34*). Resubjecting the initially obtained ^{13}C-labeled **2** to a second round of labeling yields product with 94% ^{13}C incorporation. While stoichiometric quantities of **1** are needed for optimal results, the aldehyde can be easily recovered by extraction and obtained in high purity after column chromatography in 70% yield.

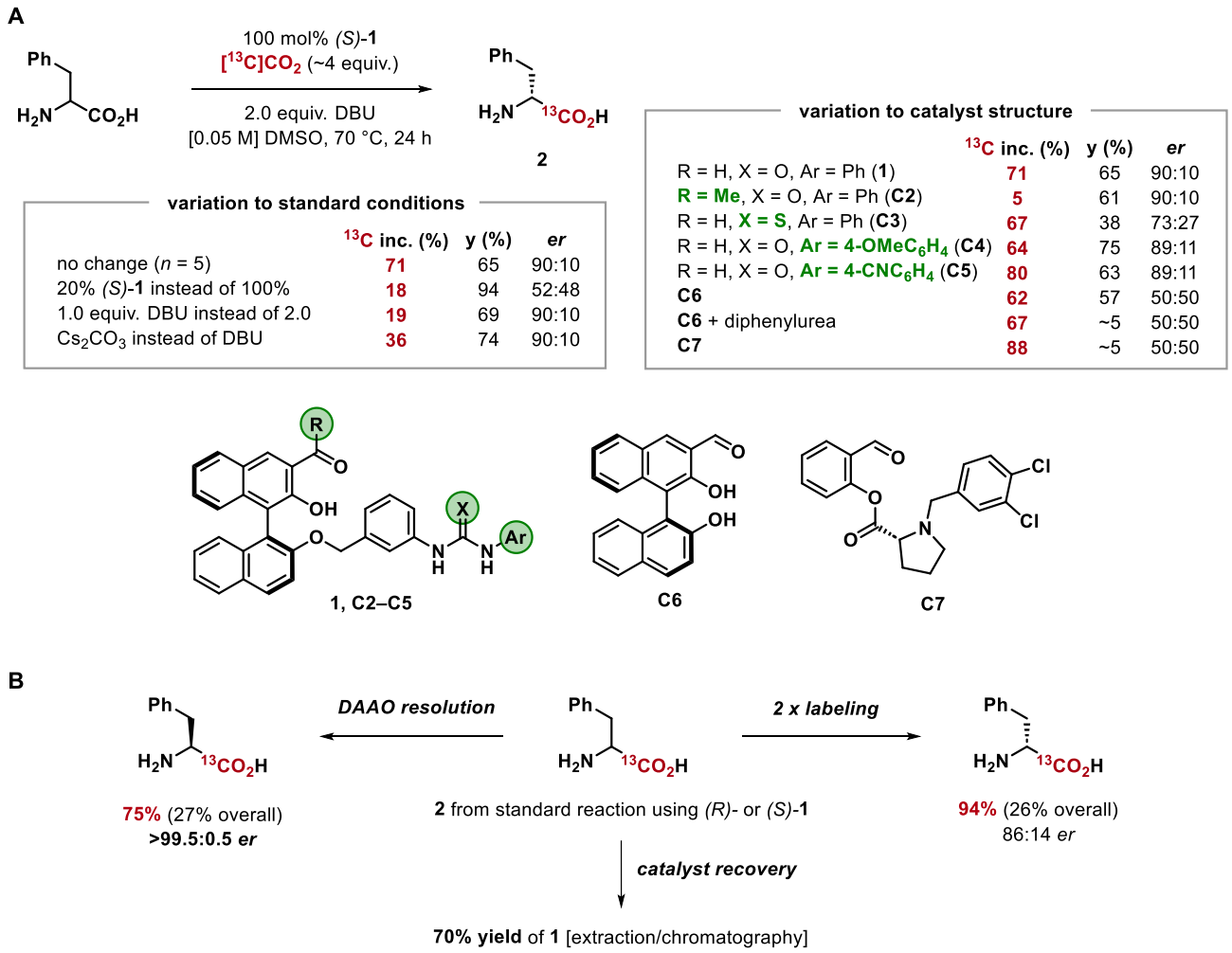

Fig. 2. Reaction optimization and product utility. (**A**) Variations to the standard conditions and catalyst structure. (**B**) **2** can be upgraded to >99.5:0.5 *er* in a subsequent enzymatic resolution or 94% ^{13}C incorporation upon re-subjection to the standard conditions. The standard catalyst **1** can be recovered after performing the enantioselective labeling experiment. DAAO = D-amino acid oxidase.

The enantioselective CIE process was amenable to a host of proteinogenic α-amino acids (Fig. 3). Substrates with aliphatic or aromatic side chains were generally well tolerated and could be labeled in 41–88% ^{13}C incorporation with up to 90:10 *er* with yields ranging from 40–64% (**2**–**7**). As shown with phenylalanine (**2**), aldehyde *(R)*-**1** can be used in the labeling/resolution of methionine (**5**), followed by subsequent enzymatic enantioenrichment using DAAO to deliver the product in 99.5:0.5 *er*. Various proteinogenic α-amino acids with acidic, basic, or neutral polar side chains were labeled productively in 32–87% ^{13}C incorporation with up to 88:12 *er* (**8**–**11**), although poor enantioselectivity is observed with glutamic acid (**11**). Arginine (**9**) and glutamine (**10**) displayed good enantioselectivity under modified conditions. Limitations of proteinogenic

substrates include amino acids with β-branched and/or potentially nucleophilic side chains, where <10% ^{13}C incorporation and <60:40 *er* was observed in all cases (**12**–**16**, see the SI for additional unsuccessful substrates).

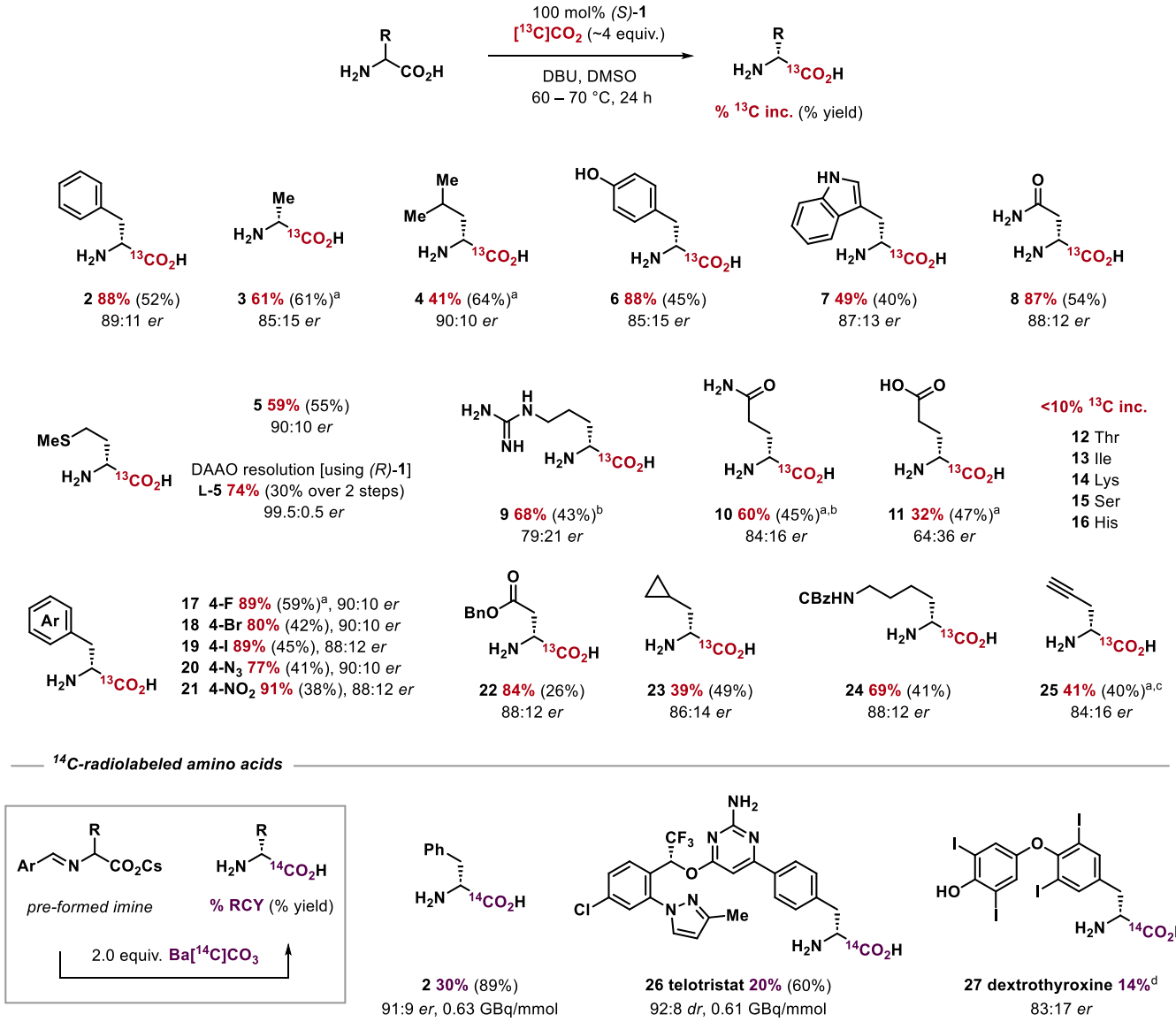

Fig. 3. ^{13}C reaction scope and ^{14}C-radiolabeling application. Unless otherwise noted, yields are of isolated material. [a] Calibrated ^{1}H NMR yield. [b] Reaction conducted at 60 °C. [c] Reaction conducted starting from the pre-formed imine carboxylate, using Cs_2CO_3 at 60 °C for 16 h. [d] Radio-HPLC yield. RCY = radiochemical yield.

The CIE protocol also tolerated a handful of non-natural α-amino acids with potentially reactive functionalities including phenylalanine derivatives containing fluoride, bromide, iodide, and nitro groups (**17**–**19**, **21**). High levels of ^{13}C incorporation (80–91%) were observed for these

substrates under the standard conditions with a minimum *er* value of 88:12. Additionally, azido phenylalanine derivative **20** (AzF) underwent productive labeling (77% ^{13}C incorporation) and resolution (90:10 *er*); this product could be potentially valuable in bioconjugation reactions (*35*). Protected amino acids β-benzyl aspartic acid (**22**) and ε-carbobenzyloxy lysine (**24**) underwent efficient ^{13}C-labeling (69–84% isotope incorporation) with *er* values of 88:12 for both products. Aliphatic non-natural derivatives that were labeled successfully under the standard conditions included cyclopropylalanine **23** (39% ^{13}C incorporation, 86:14 *er*) and propargylglycine **25** (41% ^{13}C incorporation, 84:16 *er*), the latter which bears a potentially reactive alkyne.

The standard CIE conditions were readily adapted to accommodate the ^{14}C-radiolabeling of both simple α-amino acids and complex derivatives. [^{14}C]CO_2 could be generated quantitatively from 2 equivalents of Ba[^{14}C]CO_3 and subsequently used in the enantioselective CIE of [^{14}C]**2** (30% radiochemical yield (RCY), 0.63 GBq/mmol, 91:9 *er*). Starting from the pre-formed imine carboxylate salt of **1** was necessary to achieve higher levels of radioisotope incorporation, and lowering the equivalents of DBU resulted in greater isolated yields (89%, see the SI for additional optimization studies). As the maximum theoretical RCY for [^{14}C]**2** under these conditions is 32%, this process is shown to be efficient. Additionally, the enantioselective CIE protocol was effective in the late-stage radiolabeling of drug molecules telotristat (**26**, 20% RCY, 92:8 *dr*, 0.61 GBq/mmol) and dextrothyroxine (**27**, 14% RCY, 83:17 *er*). The specific activity values of the isolated ^{14}C-radiolabeled products ([^{14}C]**2**, 3.80 MBq/mg and **26**, 1.10 MBq/mg) are suitable for ADME studies (>0.74 MBq/mg typically needed) (*18, 36*) and are near the preferred specific activity values for metabolite quantitation in agrochemical studies (5 MBq/mg) (*2*).

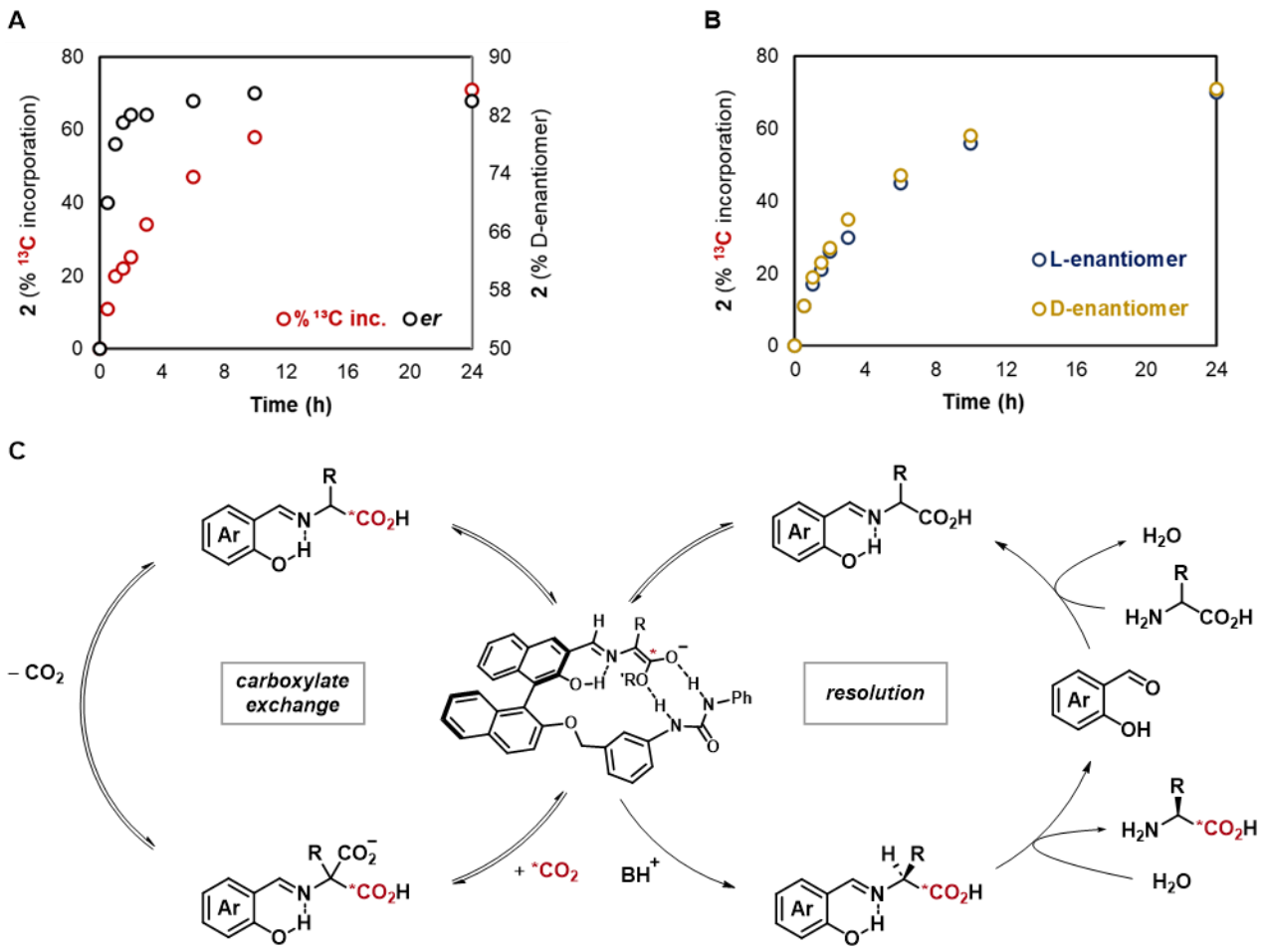

Fig. 4. Reaction progress kinetic analysis and mechanistic hypothesis. (**A**) Reaction kinetics of ^{13}C incorporation versus resolution in **2** under the standard conditions. (**B**) Reaction kinetics of ^{13}C incorporation in both enantiomers of **2** under the standard conditions. (**C**) Mechanistic proposal for simultaneous carboxylate exchange/resolution. Proton transfer steps omitted for clarity.

The mechanism of enantioselective CIE is likely composed of two separate pathways occurring simultaneously; carboxylate exchange and resolution. Reaction progress kinetic analysis of **2** under the standard conditions revealed that a near-equilibrium *er* of 85:15 is reached within the first hour of the reaction, while equilibrium ^{13}C incorporation (~80%) is gradually reached over a period of 24 hours (Fig. 4A. Note: terminal values of incorporation and *er* observed during kinetic analysis are slightly lower due to $[^{13}C]CO_2$ loss during sampling as well as crude sample racemization). Questioning whether the reaction could potentially undergo enantioselective carboxylation or decarboxylation, the rate of resolution of **2** was tested under the standard conditions using N_2 instead of $[^{13}C]CO_2$. Similar rates of resolution and terminal *er* values were observed (see the SI for additional kinetic plots). Furthermore, the extent of isotope

incorporation in either enantiomer of **2** is the same under the standard conditions (Fig. 4B), suggesting carboxylate exchange is productive in either diastereomeric imine complex and likely produces racemic iminomalonate in both cases. Resolution is achieved in a separate, faster cycle. It is probable that the amino acid remains bound to the chiral aldehyde throughout the course of the reaction, since poor *er* is achieved when using 20 mol% **1** (52:48 *er*), but the catalyst can be recovered in high yield (70%) upon quenching the reaction under the standard conditions.

A mechanistic proposal is provided in Figure 4C. Condensation between the α-amino acid and chiral aldehyde generates the corresponding imine which possesses a resonance-assisted hydrogen bond (RAHB), thus lowering the acidity of the imino acid α-proton (*37*). The imine undergoes deprotonation to form a reactive enolate intermediate which is hydrogen bonding to itself through the urea linker. This enolate intermediate can either be carboxylated or undergo resolution; both processes are occurring simultaneously, although resolution is more rapid. For the carboxylation pathway, the enolate intermediate reacts with $*CO_2$ to form an iminomalonate intermediate which is prone to monodecarboxylation (*38*). Decarboxylation of the iminomalonate regenerates the reactive enolate intermediate. For the resolution pathway, the enolate will be protonated diastereoselectively, where the selectivity is driven by the avoidance of steric clash between the imine proton and the amino acid R-group, resulting in preferential protonation of one of the faces of the planar enolate intermediate (*30*).

The concept reported here leveraging dual CIE/resolution for enantioselective processes should have immediate application and further guide stereoselective isotope exchange protocols.

References and Notes

1. C. S. Elmore, R. A. Bragg, Isotope chemistry; a useful tool in the drug discovery arsenal. *Bioorg. Med. Chem. Lett.* **25**, 167–171 (2015).
2. V. Derdau *et al.*, The Future of (Radio)-Labeled Compounds in Research and Development of the Life Science Industry. *Angew. Chem. Int. Ed.* **62**, e202306019 (2023).
3. J. D. Neufeld, M. Wagner, J. C. Murrell, Who eats what, where and when? Isotope-labelling experiments are coming of age. *ISME J.* **1**, 103–110 (2007).
4. J. Atzrodt, V. Derdau, W. J. Kerr, M. Reid, C−H Functionalisation for Hydrogen Isotope Exchange. *Angew. Chem. Int. Ed.* **57**, 3022–3047 (2018).
5. S. Kopf *et al.*, Recent Developments for the Deuterium and Tritium Labeling of Organic Molecules. *Chem. Rev.* **122**, 6634–6718 (2022).
6. G. Prakash, N. Paul, G. A. Oliver, D. B. Werz, D. Maiti, C–H deuteration of organic compounds and potential drug candidates. *Chem. Soc. Rev.* **51**, 3123–3163 (2022).
7. R. Pony Yu, D. Hesk, N. Rivera, I. Pelczer, P. J. Chirik, Iron-catalysed tritiation of pharmaceuticals. *Nature* **529**, 195–199 (2016).
8. Y. Y. Loh *et al.*, Photoredox-catalyzed deuteration and tritiation of pharmaceutical compounds. *Science* **358**, 1182–1187 (2017).
9. W. N. Palmer, P. J. Chirik, Cobalt-Catalyzed Stereoretentive Hydrogen Isotope Exchange of C(sp^3)–H Bonds. *ACS Catal.* **7**, 5674–5678 (2017).
10. C. Taglang *et al.*, Enantiospecific C–H Activation Using Ruthenium Nanocatalysts. *Angew. Chem. Int. Ed.* **54**, 10474–10477 (2015).
11. L. V. A. Hale, N. K. Szymczak, Stereoretentive Deuteration of α-Chiral Amines with D_2O. *J. Am. Chem. Soc.* **138**, 13489–13492 (2016).
12. V. Babin, F. Taran, D. Audisio, Late-Stage Carbon-14 Labeling and Isotope Exchange: Emerging Opportunities and Future Challenges. *JACS Au* **2**, 1234–1251 (2022).
13. A. Labiche, A. Malandain, M. Molins, F. Taran, D. Audisio, Modern Strategies for Carbon Isotope Exchange. *Angew. Chem. Int. Ed.* **62**, e202303535 (2023).
14. K. Hinsinger, G. Pieters, The Emergence of Carbon Isotope Exchange. *Angew. Chem. Int. Ed.* **58**, 9678–9680 (2019).
15. O. Jacobson, D. O. Kiesewetter, X. Chen, Fluorine-18 Radiochemistry, Labeling Strategies and Synthetic Routes. *Bioconjug. Chem.* **26**, 1–18 (2015).

16. D. Kong, P. J. Moon, E. K. J. Lui, O. Bsharat, R. J. Lundgren, Direct reversible decarboxylation from stable organic acids in dimethylformamide solution. *Science* **369**, 557–561 (2020).
17. G. Destro *et al.*, Transition-Metal-Free Carbon Isotope Exchange of Phenyl Acetic Acids. *Angew. Chem. Int. Ed.* **59**, 13490–13495 (2020).
18. C. Kingston *et al.*, Direct Carbon Isotope Exchange through Decarboxylative Carboxylation. *J. Am. Chem. Soc.* **141**, 774–779 (2019).
19. G. Destro *et al.*, Dynamic Carbon Isotope Exchange of Pharmaceuticals with Labeled CO_2. *J. Am. Chem. Soc.* **141**, 780–784 (2019).
20. V. Babin *et al.*, Photochemical Strategy for Carbon Isotope Exchange with CO_2. *ACS Catal.* **11**, 2968–2976 (2021).
21. D. Kong *et al.*, Fast Carbon Isotope Exchange of Carboxylic Acids Enabled by Organic Photoredox Catalysis. *J. Am. Chem. Soc.* **143**, 2200–2206 (2021).
22. O. Bsharat *et al.*, Aldehyde-catalysed carboxylate exchange in α-amino acids with isotopically labelled CO_2. *Nat. Chem.* **14**, 1367–1374 (2022).
23. D. R. Gauthier, Jr., N. R. Rivera, H. Yang, D. M. Schultz, C. S. Shultz, Palladium-Catalyzed Carbon Isotope Exchange on Aliphatic and Benzoic Acid Chlorides. *J. Am. Chem. Soc.* **140**, 15596–15600 (2018).
24. S. W. Reilly, Y.-h. Lam, S. Ren, N. A. Strotman, Late-Stage Carbon Isotope Exchange of Aryl Nitriles through Ni-Catalyzed C–CN Bond Activation. *J. Am. Chem. Soc.* **143**, 4817–4823 (2021).
25. M. Feng *et al.*, Direct Carbon Isotope Exchange of Pharmaceuticals via Reversible Decyanation. *J. Am. Chem. Soc.* **143**, 5659–5665 (2021).
26. N. Wang *et al.*, New Approved Drugs Appearing in the Pharmaceutical Market in 2022 Featuring Fragments of Tailor-Made Amino Acids and Fluorine. *Molecules* **28**, 3651 (2023).
27. M. Muttenthaler, G. F. King, D. J. Adams, P. F. Alewood, Trends in peptide drug discovery. *Nat. Rev. Drug Discov.* **20**, 309–325 (2021).
28. R. Voges, J. R. Heyes, T. Moenius, *Preparation of Compounds Labeled with Tritium and Carbon-14* (John Wiley & Sons. Ltd, 2009).
29. A. Dell'isola *et al.*, Synthesis of carbon-14–labelled peptides. *J. Label. Compd. Radiopharm.* **62**, 713–717 (2019).

30. H. Park *et al.*, Bioinspired Chemical Inversion of L-Amino Acids to D-Amino Acids. *J. Am. Chem. Soc.* **129**, 1518–1519 (2007).
31. R. Nandhakumar *et al.*, Effects of ring substituents on enantioselective recognition of amino alcohols and acids in uryl-based binol receptors. *Tetrahedron* **64**, 7704–7708 (2008).
32. J. Chin, D. C. Kim, H.-J. Kim, F. B. Panosyan, K. M. Kim, Chiral Shift Reagent for Amino Acids Based on Resonance-Assisted Hydrogen Bonding. *Org. Lett.* **6**, 2591–2593 (2004).
33. H. Park *et al.*, Stereoconversion of Amino Acids and Peptides in Uryl-Pendant Binol Schiff Bases. *Chem. Eur. J.* **14**, 9935–9942 (2008).
34. R. Fernández-Lafuente, V. Rodriguez, J. M. Guisán, The coimmobilization of D-amino acid oxidase and catalase enables the quantitative transformation of D-amino acids (D-phenylalanine) into α-keto acids (phenylpyruvic acid). *Enzyme Microb. Technol.* **23**, 28–33 (1998).
35. D. Guan, Y. Kurra, W. Liu, Z. Chen, A click chemistry approach to site-specific immobilization of a small laccase enables efficient direct electron transfer in a biocathode. *Chem. Commun.* **51**, 2522–2525 (2015).
36. J. Roosendaal, H. Rosing, J. H. Beijnen, Combining Isotopic Tracer Techniques to Increase Efficiency of Clinical Pharmacokinetic Trials in Oncology. *Drugs R D* **20**, 147–154 (2020).
37. R. Fu, S. M. So, A. J. Lough, J. Chin, Hydrogen Bond Assisted L to D Conversion of α-Amino Acids. *Angew. Chem. Int. Ed.* **59**, 4335–4339 (2020).
38. B. P. Callahan, R. Wolfenden, Charge Development in the Transition State for Decarboxylations in Water: Spontaneous and Acetone-Catalyzed Decarboxylation of Aminomalonate. *J. Am. Chem. Soc.* **126**, 4514–4515 (2004).

Acknowledgements

We thank Randy Whittal, Béla Reiz, and Angelina Morales-Izquierdo for assistance with mass spectrometry analyses related to ^{13}C-labeling experiments, as well as Claudia Loewe and Martin Sandvoß for assistance with mass spectrometry and liquid scintillation analyses related to ^{14}C-labeling experiments. Svetlana Grigoryan is thanked for assistance with the synthesis of **1**. Gareth Lambkin is thanked for assistance with DAAO-catalyzed reactions.

Funding: Support was provided by NSERC Canada (RGPIN-2019-06050 and RGPAS-2019-00051 to R.J.L., CGS-D Fellowship to M.G.J.D.), the Canadian Foundation for Innovation (IOF 32691 to R.J.L.), Mitacs (Mitacs-Accelerate International Fellowship to M.G.J.D. and R.J.L.), the Province of Alberta (AGES Fellowship to M.G.J.D., AGES Fellowship to O.B.), and the Killam Trusts (IWK Fellowship to M.G.J.D.).

Author contributions: M.G.J.D. conducted optimization, ^{13}C and ^{14}C scope, mechanistic studies, and co-wrote the manuscript. O.B. optimized the reaction and performed ^{13}C scope studies. A.S. conducted ^{14}C scope and optimization. V.D. supervised and directed ^{14}C studies. R.J.L. supervised the project, developed the concept of the work, and co-wrote the manuscript. All authors contributed to data analysis and editing of the manuscript.

Competing interests: A.S. and V.D. are employees of Sanofi Germany and may hold shares or options of the company. The remaining authors declare no competing interests.

Data and materials availability: All experimental data are available in the accompanied supplementary materials.